Proceedings of ASME Turbo Expo 2012
GT2012
June 11-15, 2012, Copenhagen, Denmark

GT2012-69151

IMPELLER-DIFFUSER INTERACTION IN CENTRIFUGAL COMPRESSORS

Chris Robinson
PCA Engineers Limited
Lincoln, UK

Michael Casey
PCA Engineers Limited, Lincoln, UK and
ITSM, University of Stuttgart

Brad Hutchinson
ANSYS, Inc.
Waterloo, ON, Canada

Robin Steed
ANSYS, Inc.
Waterloo, ON, Canada

ABSTRACT

This paper reports several CFD analyses of a centrifugal compressor stage with a vaned diffuser at high pressure ratio using different techniques to model the rotor-stator interaction. A conventional steady stage calculation with a mixing-plane type interface between the rotor and stator was used as a baseline. This simulation gave excellent agreement with the measured performance characteristics at design speed, demonstrating the ability of the particular steady simulation used to capture the essential features of the blockage interaction between the components.

A full annulus simulation using a transient rotor-stator interaction (TRS) method was then used at the peak efficiency point to obtain a fully unsteady reference solution, and this predicted a small increase in peak efficiency. Finally, a computationally less expensive unsteady calculation using a Time Transformation (TT) method was carried out. This gave similar results to the fully transient calculation suggesting that this is an acceptable approach to estimate unsteady blade loading from the interaction.

The impeller diffuser spacing was then reduced from 15 to 7% of the impeller tip radius using the more affordable TT approach. This identified an increase in efficiency of 1% and predicted unsteady pressure fluctuations in the impeller which were 116% higher with the closely spaced diffuser.

NOMENCLATURE

b	Channel width (m)
d	Diameter (m)
C_p	Static pressure coefficient
D	Impeller tip diameter (m)
H	Total enthalpy (J/kg)
k	Turbulent kinetic energy (J)
Mu	Tip-speed Mach number ($U/\sqrt{[\gamma R T_{01}]}$)
R	Gas constant (J/kgK)
Re_D	Reynolds number based on diameter
SST	Shear Stress Transport turbulence model
T_{01}	Total temperature at inlet (K)
TBR	Transient Blade Row
TRS	Transient Rotor Stator
TT	Time Transformation
U	Tip speed (m/s)
V	Inlet volume flow (m^3/s)
ε	tip clearance (m)
η	Isentropic Efficiency
ϕ	Flow coefficient (V/UD^2)
ψ	Work coefficient ($\Delta H/U^2$)
γ	Ratio of specific heats
ΔH	Total enthalpy rise (J/kg)
$\Delta p/q$	Non-dimensional pressure difference normalized by dynamic head

INTRODUCTION

Centrifugal compressor stages for a wide range of applications comprise an impeller closely coupled to a vaned diffuser. The radial gap between the impeller and diffuser typically varies between about 5 and 15% of the impeller tip radius which is only a small fraction of the chord of the two blade rows. It is known that to maximize efficiency the rotor-stator spacing should be reduced, but at very close spacing there is a strong probability that the impeller will be excited mechanically as it passes through the static pressure field of the diffuser. A design at increased radial spacing will reduce the mechanical excitations, but the classical work of Dean and Senoo **[1]** in vaneless diffusers shows that, although the mixing of the wakes and unsteady flow leaving the impeller takes place rapidly, it will still not have fully mixed out ahead of the diffuser, so that unsteady effects may still be relevant.

The present work examines this problem using different steady and unsteady CFD techniques. The work concentrates on stages with a pressure ratio above 4 in air (which requires an impeller tip-speed Mach number typically above 1.4).

For these applications which can be found in turbochargers, refrigeration compressors and gas turbines most centrifugal stages feature an impeller with a vaned diffuser as shown in **fig 1**.

Over recent years the improvement in accessibility to high fidelity CFD has been utilized to good effect in design improvements leading separately to both impeller efficiency **[2]** and diffuser pressure recovery and loss reduction **[3]** in stages of this type. The matching of the impeller to the diffuser is also critical in achieving optimal stage performance, simply on a one-dimensional basis. In fact, Cumpsty **[4]** states that mismatching is far more common as a cause of poor performance with high pressure ratio machines than the details of impeller or diffuser vane shape. It is crucially important to predict the correct diffuser inlet blockage when considering the matching of the impeller and diffuser and in developing the design of either blade.

For this purpose it is general practice to make use of steady calculations and the pragmatic solution is to use a "Stage Interface" or "Mixing Plane" method which in some manner mixes the flow circumferentially as it passes from the rotating to the stationary domains.

This approach has been very successful in achieving well-matched designs at significant radial spacing but provides no information on the unsteady interactions. Unsteady information requires a transient rotor-stator (TRS) calculation but, since blade numbers are usually deliberately chosen to avoid common multiples, to set-up an accurate transient calculation with fewer than full-360° coverage is not normally practicable.

In the last fifteen years, new transient blade row (TBR) methods have been developed which are capable of reproducing the transient behaviour of a full wheel from the simulation of a few passages. These methods promise greater simulation fidelity for unsteady flows at a much lower computational cost. Furthermore, TBR methods, such as Time Transformation (TT), also return information on pressure fluctuations which may be used to assess the mechanical impact of radial spacing on the compressor design.

The diffuser experiences high levels of inlet absolute Mach number with a high level of swirl and the operating range of this row often limits the map width of the stage. For some applications it is standard practice to optimize the diffuser for a part-speed condition, while the impeller is designed to cope with the maximum speed and flow. This places a high reliance on CFD in these days where the pressures to reduce development cost and timescales are acute.

The influence of spacing between adjacent blade rows on efficiency has been the subject of some detailed studies, both in axial and radial machinery.

There is a body of literature from respected sources that suggests that there is an efficiency advantage from a relatively small radial gap between the impeller and diffuser of centrifugal compressor stages, below the level that would be considered relatively safe from the point of view of mechanical excitation. For example Rodgers **[5]** published empirical results showing an optimum diffuser inlet radius ratio of about 112% in a study where care was taken to preserve diffuser throat area. Shum et al. **[6]** reported a comprehensive theoretical study applying transient CFD to a stage with varying spacing (105% of impeller tip radius, 109% and a vaneless diffuser) concluding that the beneficial effects derive mainly from reduced blockage and reduced slip factor accruing from changes to the clearance flow within the impeller. An optimum of about 109% was suggested. Ziegler et al. **[7, 8]** attempted a systematic study in a rig where the diffuser vanes could be moved radially over a range of 104 to 118%, publishing comprehensive measurements including laser anemometry and overall performance. The general consensus seems to be that an optimum radius ratio from the performance perspective lies somewhere in the range between 105 and 112%.

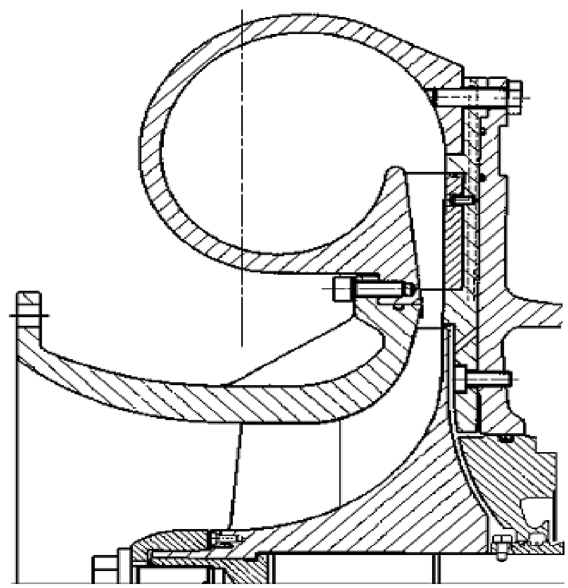

Figure 1 Section of a high pressure turbocharger stage

However, the unsteady pressure field experienced by the rotor as it passes the diffuser vanes is an important source of mechanical excitation. Fatigue failures through this mechanism are not widely reported but are well-known. A Campbell analysis of an impeller using finite element techniques will give an indication of speeds where excitation may occur, and the standard approach in developing a design is to try to manipulate the impeller natural frequency levels with subtle changes to blade camber or thickness or local disc thickness, and to affect the excitation frequencies by appropriate selection of diffuser vane count. With continuously variable speed machines, such as turbochargers, operation at some conditions where resonance may occur is inevitable and here it is essential to ensure that sufficient natural damping is available in the vanes to avoid unwanted dynamic stresses.

More recent developments in multi-physics analysis combine CFD and FE interactively to be able to assess the level of excitation but these are very demanding of computing resource, often requiring full 360° modeling.

Whilst this could be practicable for checking a final design, for designs to be fully optimized taking aerodynamic and mechanical factors into consideration there is a need for a more computationally convenient approach.

A compressor stage typical of those found in turbochargers in rail traction or power generation, or recuperated micro gas turbines is briefly described in section 1. The computational methods are described in section 2, particularly contrasting the steady-state solutions with the full transient rotor-stator (TRS) method with the more affordable time transformation (TT) approach. Section 3 gives the results of the steady analysis of the original compressor with a vaned diffuser with a radial inlet at 115% of the impeller outlet and describes the development of a closer-spaced diffuser vane with a radial spacing of 107%.

Section 4 reports the more sophisticated transient analyses, looking for read-across to the earlier publications on this topic and also comparing the TT and TRS results with those from the standard steady stage analysis that is believed to be the most common approach in developing new designs.

THE COMPRESSOR STAGE

The compressor stage that formed the basis of the present study is illustrated in **fig 2** and key design parameters are summarized in **table 1**. The impeller blades are flank-milled and the diffuser has an aerodynamic profile of constant spanwise vane section. The stage as tested includes a volute but this was not modeled in this CFD study. The tests were carried out in a dedicated compressor test stand in an industrial environment, with great attention to instrumentation giving an accuracy level of better than 1%.

Parameter	Symbol	Value
Flow coefficient	$\phi = V/UD^2$	0.094
Work coefficient	$\psi = \Delta H/U^2$	0.72
Tip-speed Mach number	Mu	1.54
Number of rotor blades		11+11
Number of diffuser vanes		17
Axial clearance to span ratio	ε/b	0.02
Diffuser leading edge ratio	d/D	115%
Reynolds number	Re_D	1.23×10^7

Table 1 Compressor non-dimensional design parameters

COMPUTATIONAL METHODS

The approach taken in this work was to use a variety of CFD methods to study the effect of impeller-diffuser spacing in a centrifugal stage.

Predictions were obtained for both the original configuration with a radius ratio of 115% and the reduced spacing configurations (107%). All grids were fully hexahedral and were generated using the automated topology and mesh (ATM) method in ANSYS TurboGrid Release 14.0. Simulations were performed with ANSYS CFX Release 14.0 **[9]** using the "High Resolution" advection scheme for all equations except turbulence, for which a first order upwind scheme was used. High Resolution advection is a bounded second order scheme. For turbulence, the SST turbulence model of Menter **[15]** was employed because of its acknowledged success in modeling flows in an adverse pressure gradient.

Figure 2 Photograph of the subject stage

The first step was to carry out a baseline calculation with the steady-state "Stage Interface" method **[9],** which uses a mixing-plane interface approach. The initial development of this procedure is described in the paper of Denton **[10]** and some information about the development and usage of the current implementation is given in the papers **[11, 12, 13 and 17]**. There are two special features of this implementation. The first is is that it includes a virtual 2D control surface between the upstream and downstream regions of the interface, so that the circumferential static pressure variations in both regions are determined by the local domain and only the mean value is determined by the circumferential averaging of fluxes that takes place there. Secondly it allows flow to traverse the interface in both directions.

Despite the circumferential averaging of the flow at the interface, typically located mid-way between the impeller trailing edge and diffuser leading edge, global mass, momentum and energy are conserved across the interface, except that the global entropy increases. This entropy increase is due to the averaging process that mixes out the impeller wake, see Giles [**14].** Consequently, only the circumferentially averaged flow field is transmitted to the diffuser and this simplification represents the primary approximation of the method. Nevertheless, the average spanwise profile of the flow is maintained. This method is now a standard tool that serves the design process well. Here the method is used to simulate the flow at a number of operating points ranging from choke to near surge along a line of constant speed.

A major attraction is its computational efficiency, since the circumferential averaging enables representation of each blade row by a single blade passage and automatically includes the matching of the components without separate calculations for each.

An alternative procedure is to use a so-called frozen-rotor interface in which all circumferential velocities at the rotor stator interface are simply changed by the local blade speed. This is not used here.

Fully transient calculations were performed in an effort to more accurately capture the detailed flow physics, and in particular the passage of the impeller wake across the diffuser inlet. It should be noted at the outset that the wake in the relative frame of the impeller becomes a jet in the absolute frame of the diffuser, as can be seen in the PIV measurements published by Cukerel et al. [**16**]. Two approaches were used. The transient rotor-stator (TRS) method was used to obtain a full annulus simulation at the peak efficiency point. While fully capturing the detailed physics, the simulation is computationally very expensive since all flow passages (11 in the impeller, 17 in the diffuser) were simulated resulting in a very large computational mesh with associated large computational requirements (RAM and disk).

The TRS solution serves as a reference solution, against which solutions from more economic transient methods can be compared. Here the time transformation (TT) method is used. It belongs to a family of transient blade row methods known as “transformation methods” **[17]**, which overcome the issue of unequal pitch in adjacent blade rows by transforming some quantity according to its own specific method.

The TT method was developed after the time-inclining method of Giles **[14]** but applied to the Navier-Stokes equations and implemented in a fully implicit manner. The equations are transformed in time according to the pitch ratio and relative component speeds such that periodic conditions can be applied to pitchwise boundaries, despite differences in blade count of adjacent blade rows. An advantage of the method is that it makes no assumption as to the frequency of disturbances and hence is able to capture both the imposed frequency of the blade passing as well as other flow-generated frequencies, for example the unsteady shedding of wakes **[14]**. The method is generally restricted to a single stage (2 blade rows), and also has stability limitations which restrict the pitch ratio that can be simulated. The latter restriction can be overcome by simulating more than one blade passage of one or both blade rows. In this particular instance an ensemble of two impeller and three diffuser passages satisfies the stability restrictions.

Grid density	Impeller nodes	Diffuser nodes	Grid angle	y^+ (estimated)
Coarse	141292	120226	25.6	17.0
Medium	265622	226020	20.0	4.5
Fine	518756	514120	15.2	1.5

Table 2 Stage grids (one impeller, one diffuser)

The work began with a study of solution sensitivity to grid refinement. Steady solutions for the original geometry configuration were obtained on the range of grids reported in **table 2**, the medium density mesh is illustrated in **fig 3**.

Grid quality as characterized by grid angle was generally very high, and in most regions close to orthogonal (90°), except near the impeller trailing edge in the tip gap, and only these smaller angles are reported in **table 2**. **Table 2** also indicates sufficient near wall resolution, as characterized by the y^+ values indicative of the dimensionless spacing of the near-wall grid, thus adequately resolving boundary layers, as illustrated by a portion of the mesh shown in **fig 3**.

Model	Impeller passages	Diffuser passages	Total nodes
Steady	1	1	483620
TT	2	3	1179582
TRS	11	17	6558482

Table 3 Simulation passages and overall grid sizes for the medium grid density

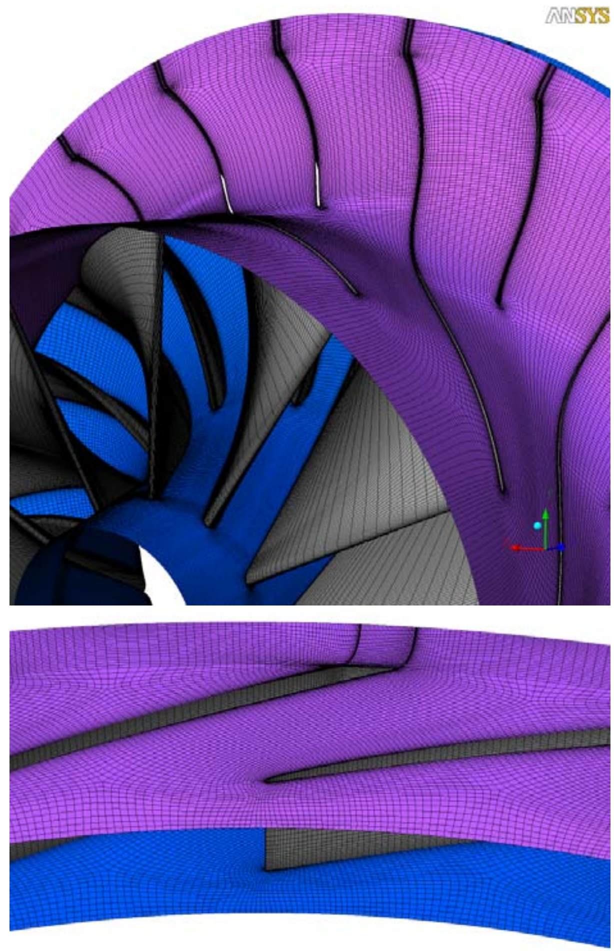

Figure 3 Medium density mesh as used in the study

All simulations used an ideal gas representation of air as the working fluid, with inlet conditions of constant total pressure, total temperature and zero inlet swirl in the absolute reference frame. For the exit, expressions were used to specify the target exit corrected mass flow.

Differences between predicted overall performance parameters on coarse, medium and fine grids were small, as can be seen from **fig 4**, which shows the predicted efficiency and work coefficient against non-dimensional flow coefficient, giving a maximum difference of 0.18% points of efficiency between the medium and fine cases.

The medium grid density was selected for all subsequent calculations. This grid density is equivalent to, or larger than, that routinely used by some of the authors in the design of similar stage configurations. The number of passages simulated and the total grid sizes for each of the simulation methods are summarized in **table 3.** For each transient simulation, a corresponding steady simulation was first obtained and used as the starting point.

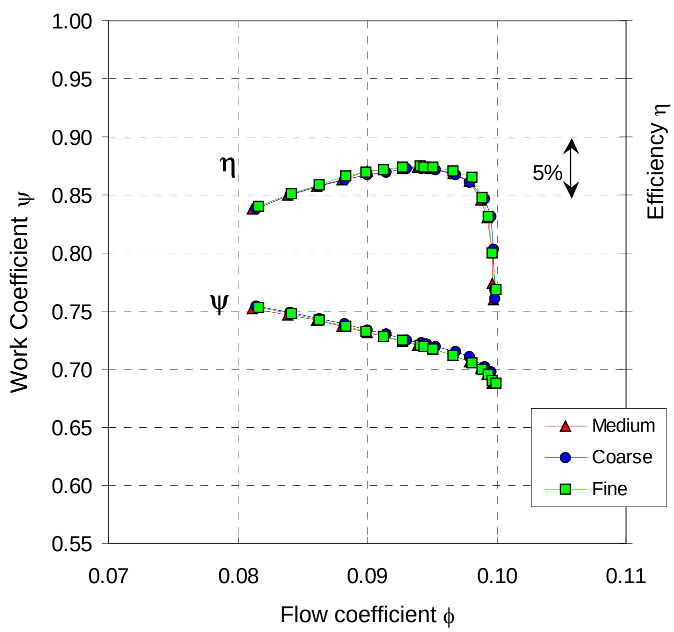

Figure 4 Results of the mesh dependency study (steady solutions)

STAGE RESULTS AND DIFFUSER DESIGN

The conventional approach used by the authors when applying CFD in support of the iterative design process is to apply the steady Stage Interface method. The baseline stage was run at a range of operating conditions between choke and the measured surge line at the nominal tip-speed Mach number of 1.54. The results are compared to test data in **fig 5**.

There is excellent agreement on choke flow and work input factor. Several definitions of efficiency are included as post-processed from the CFX results. The impeller total-total efficiency (which doesn't include the mixing loss) is clearly the highest, then the diffuser exit total-total efficiency is 5-7% lower reflecting the total pressure lost in the vaneless space and vaned diffuser. The diffuser outlet total-static efficiency is shown, about 5% below the total-total level at that plane. As mentioned earlier, the volute shown in **fig 2** was not included in the calculation model and the difference between the diffuser exit total-total and total-static efficiencies reflects the significant dynamic head at that plane. A fourth set of predicted total-total efficiencies shows the effect of an assumed loss of 30% of dynamic head in the volute, typical of values found in test analyses and predictions of these components.

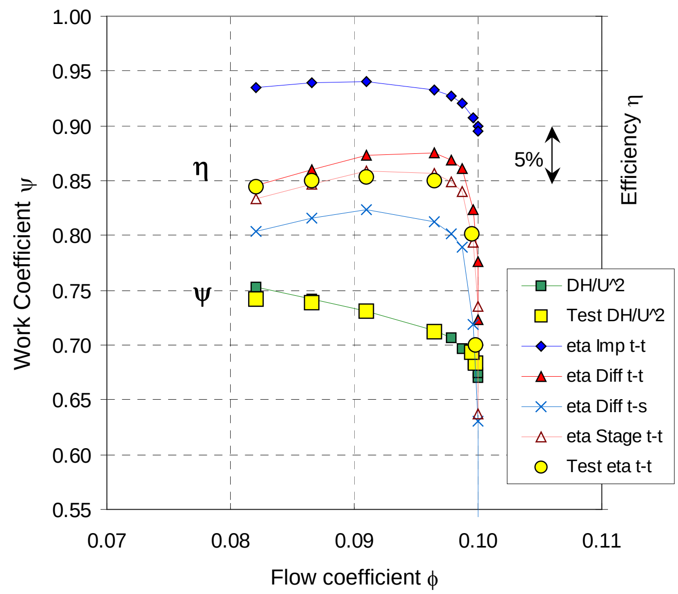

Figure 5 Predicted steady stage characteristic compared with test at a tip-speed Mach number of M=1.54

This is sufficiently close to the test values of efficiency to build confidence that the stage results, at least at this level of rotor-stator spacing, are plausible.

The original design followed the authors' extensive experience in this area and used an impeller-diffuser radius ratio of 115%. Over many years this has proved adequate to avoid the mechanical excitation mentioned above and also beneficial in that the Mach number at inlet to the diffuser falls as radius increases due to the diffusion in the vaneless/semi-vaneless space.

Diffuser design at reduced radius ratio is clearly of interest, so a new diffuser was defined at a spacing of 107%. The absolute Mach number was post-processed as a function of radius ratio from an analysis of the baseline simulation at the target peak efficiency operating point. It was then assumed that there would be no change to total temperature and pressure across the vaneless space and that the throat blockage would be similar for the two cases. Then the inverse of the ratio of the values of $M\sqrt{T_0}/AP_0$ corresponding to the Mach numbers at 107% and 115% gives a guide to a suitable throat area for the close-coupled diffuser. This suggested a 5% reduction in throat area.

The channel of the datum design was pinched to a minimum axial width at 107% radius ratio and the same meridional channel was used for the close-coupled diffuser.

A second decision to be taken was whether to allow the closer-spaced diffuser to reach the same outlet radius as the datum, or to keep a similar chord. In fact the option to maintain outlet diameter was chosen.

Diffuser vane count, maximum thickness and thickness distribution were unchanged from the baseline, as far as practicable. A comparison of the geometries is shown in **fig 6**, the baseline at 115% is in black, the closer, 107% vane is in blue.

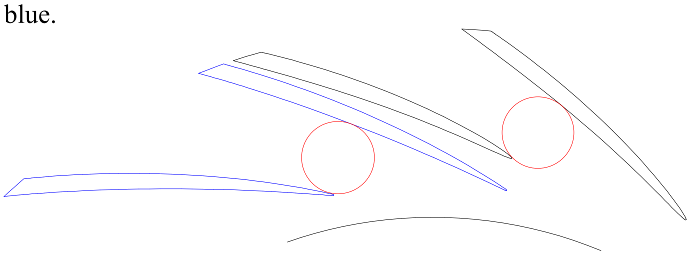

Figure 6 Diffuser geometries

The arc represents the impeller exit location and both diffusers terminate at a radius ratio of 143%. The vanes are very similar in inlet metal angle (69°) and throat width, the 5% throat area change is achieved via a narrower meridional channel. The vanes have differing degrees of divergence in the covered passage (2θ) but both are within the range applied by the authors in industrial designs.

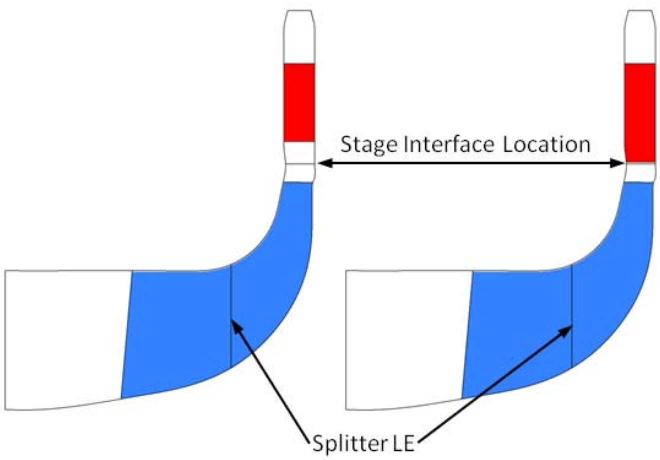

Figure 7 Meridional views of the cases analysed

NUMERICAL PREDICTIONS AND OBSERVATIONS

Fig 7 shows meridional views of the two configurations, the stage interface in both cases is at the same radius ratio so is much closer to the diffuser leading edge in the close-coupled case. The diffusers terminate at the same radial location as sketched in **fig 6**. The meridional channel was pinched slightly at outlet from the diffusers' computational domain as shown in **fig 7** to help to avoid any reverse flow on the outlet boundary.

Fig 8 shows the computed steady-state, stage overall performance results for the baseline and close-coupled diffuser. The baseline is shown with solid symbols and lines, the close-spaced diffuser with open symbols and dashed lines. The work factor seems also to be marginally higher in line with the discussion of Shum et al. **[6]**. The efficiency for the close-coupled case is similar in its peak value, but the peak is slightly closer to choke consistent with a vane operating at higher inlet Mach number.

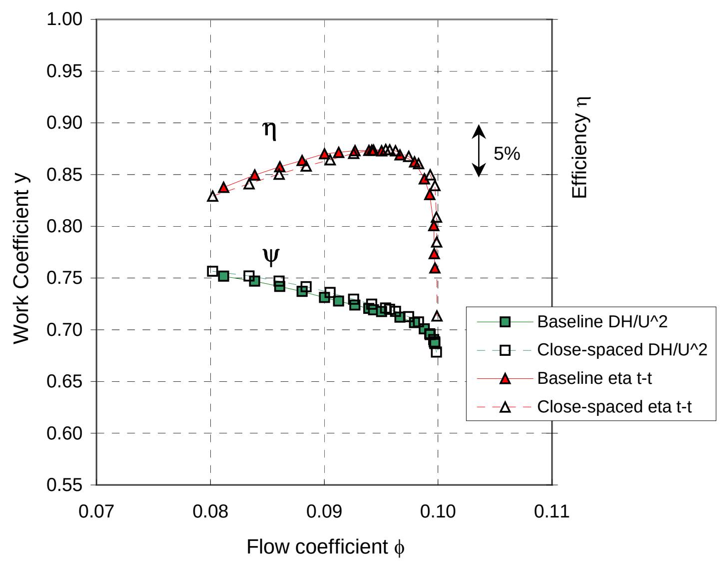

Figure 8 1D results predicted for the baseline and close-spaced diffuser – steady-state, stage interface

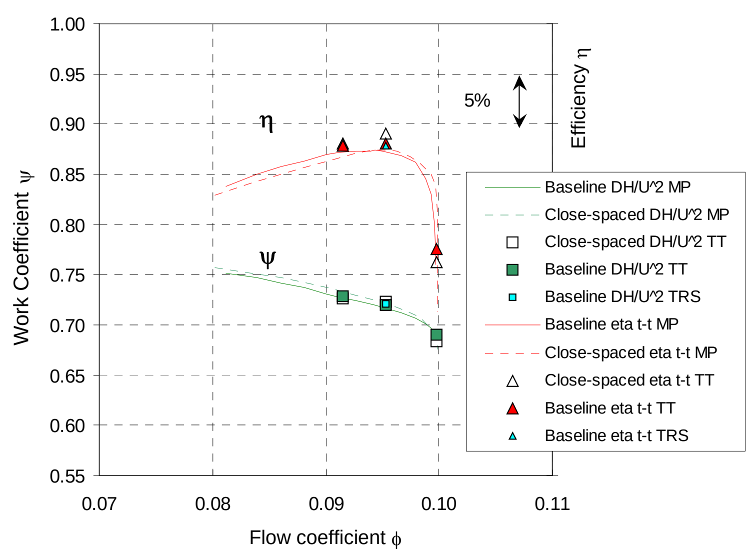

Figure 9 1D results distilled from 3D CFD predicted for the baseline and close-spaced diffuser including TT and TRS

The TT results are added in **fig 9**; only one TRS point is shown for the baseline configuration in blue.

The TT results suggest an increment in efficiency for the close-coupled diffuser and agree well on choke flow. The implication is that the steady calculations are compromised for the close-coupled case such that they don't reveal the efficiency increment seen by TT.

The TRS results (light blue symbol) agree very well with the TT results at the single operating point considered. This is very encouraging, the more affordable calculations seem not to compromise accuracy. This can be expected to read across to the close-coupled case where the steady results seem less reliable.

The following plots concentrate on the peak efficiency operating points. The baseline configuration is shown in the left hand plots, the close-coupled diffuser is shown on the right. These results are from the steady analyses.

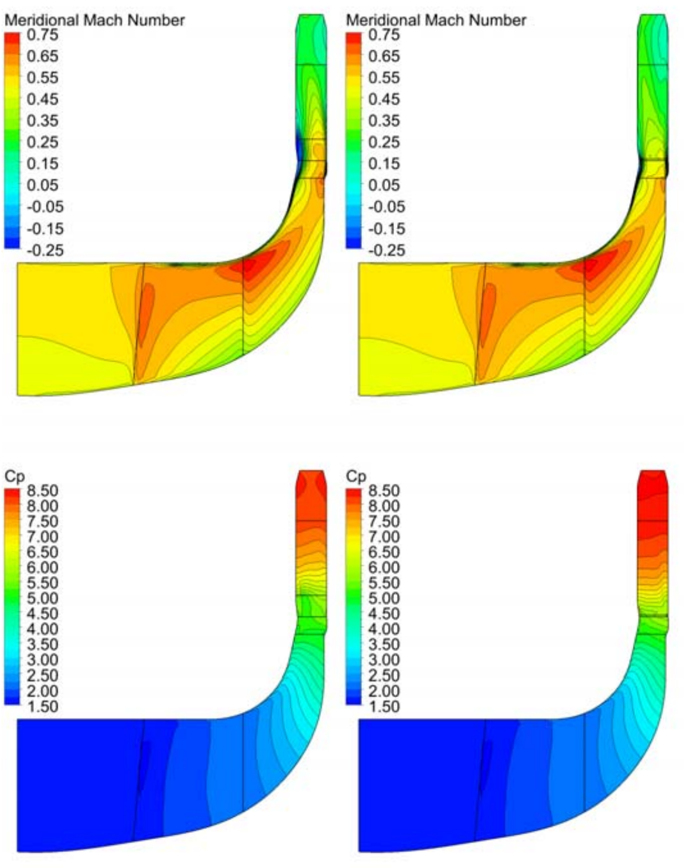

Figure 10 Distributions of mass weighted circumferential Mach number and average pressure coefficient from the steady analyses
Left: baseline (115%) Right: close-coupled (107%)

Fig 10 shows pitchwise-averaged static pressure normalised by stage inlet dynamic head (Cp) and Mach number. The flow leaving the impeller has the characteristic hub-strong profile, the tip clearance flow from the impeller having an important effect on the flow entering the diffuser, even at this comparatively low level of clearance (**table 1**).

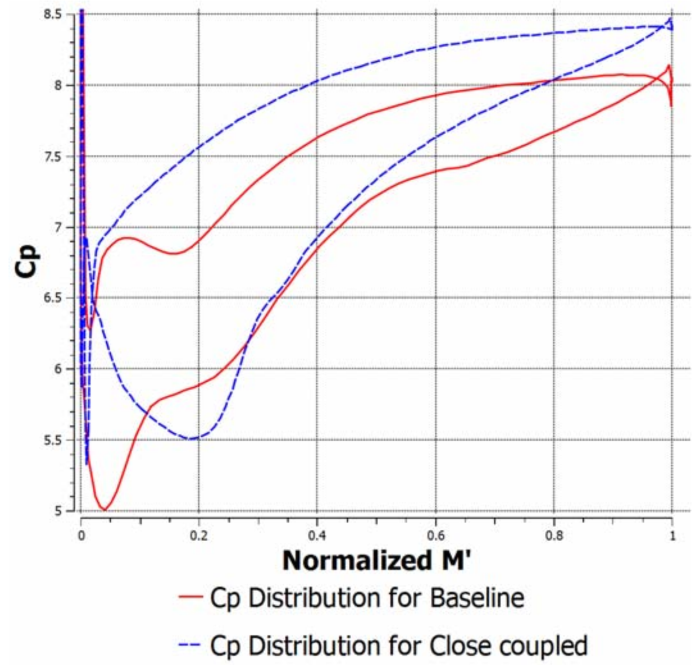

Figure 11 Diffuser mid-span static pressure distributions

Fig 11 shows the mid-span static pressure distributions for the two cases. The baseline is at higher apparent incidence judged by the leading edge loading despite having similar metal angles and common flow at exit from the impeller. This appears to be the result of the diffusion of the meridional flow caused by the diverging outer wall.

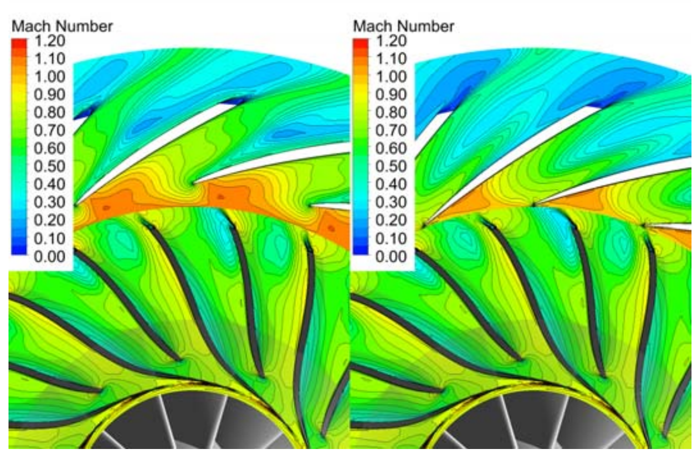

Figure 12 Relative Mach number at 50% span
Left: baseline (115%) Right: close-coupled (107%)

Fig 12 shows the mid-span relative Mach number distributions through each stage. In terms of chord-wise spacing, these highlight just how closely coupled the two blade rows are, even in the 115% baseline case. The closer diffuser seems not to suffer from an increase in the suction surface Mach number, which is one aspect which could have had a deleterious effect on the aerodynamic performance at small radial spacing.

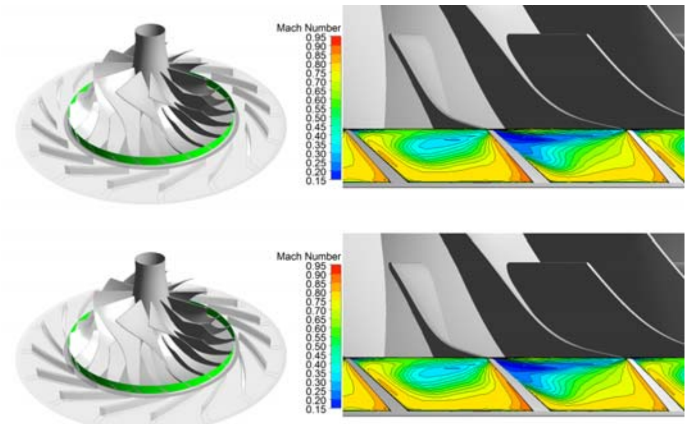

Figure 13 Impeller exit relative Mach number distribution from steady state calculation
Top: baseline (115%) Bottom: close-coupled (107%)

Shum et al **[6]** suggested that one impact of moving the diffuser closer to the impeller was a change in clearance flow. **Fig 13** shows impeller exit conditions for the two cases (baseline is uppermost).

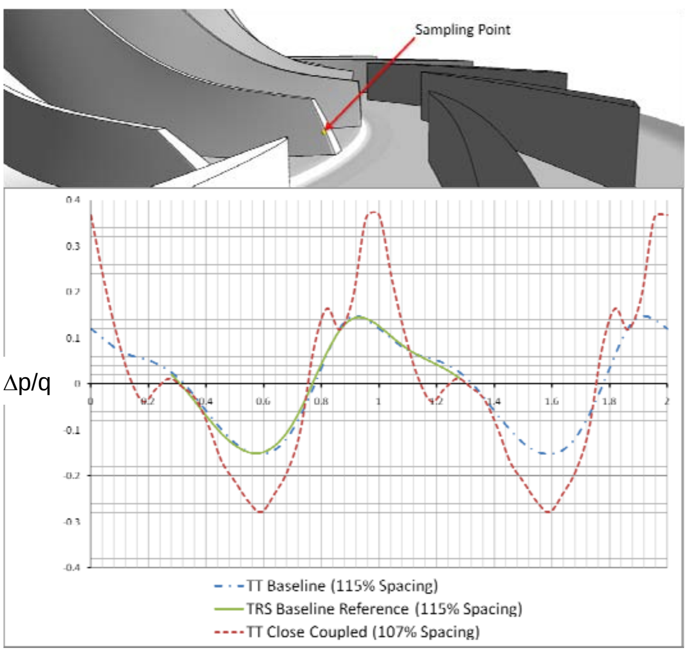

Figure 14 Blade surface pressure at impeller exit

While there is no striking difference between these plots, an integration of the clearance flow over both main blades and splitters revealed that the closer spaced diffuser case had 4.3% less flow passing over the blade tips. This sounds small but is in the direction likely to improve performance. This could also be the explanation for the small increase in work noted with respect to **fig 8**.

Fig 14 shows the surface pressure distribution at a point on the blades at impeller mid-span from the TT and reference solutions near peak efficiency.

The quantity plotted is the difference between the instantaneous static pressure and the average across a revolution, normalized by the mean dynamic head at impeller exit. The horizontal axis is the impeller blade passing period, with two periods shown. The pressure profile predicted for the baseline configuration by the TT method shows good agreement with the reference solution.

Reducing the spacing from 115% to 107% has resulted in an increase in the amplitude of the pressure fluctuations by 116% at this location. To be able to deploy close-coupled diffusers without compromising mechanical robustness it is clearly essential to evaluate the mechanical response to these fluctuations.

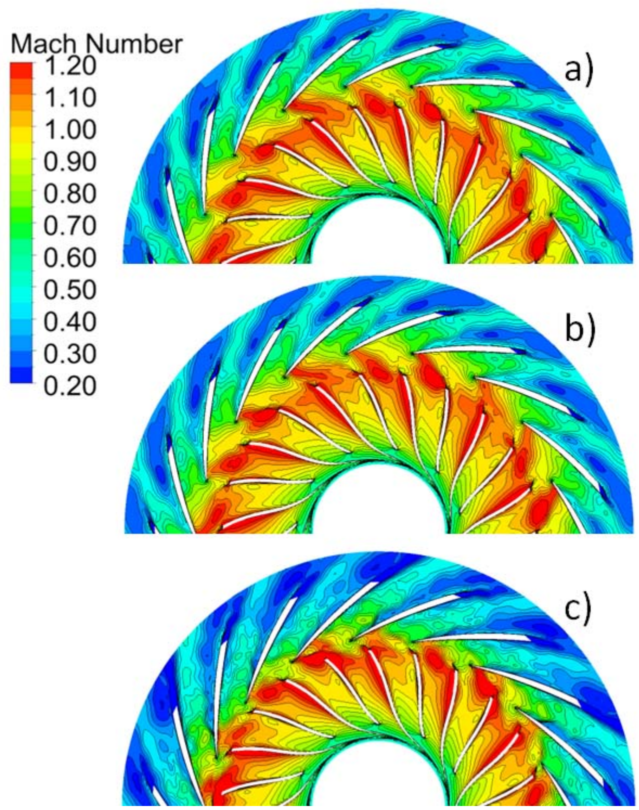

Figure 15 Absolute Mach number from transient calculations at mid-span. a) Baseline TRS results, 115% spacing, b) Baseline TT results, 115% spacing, c) Close-coupled TT results, 107% spacing

Fig 15 shows more detail of the differences in absolute Mach number experienced by the baseline and close-spaced blades at mid-span. **Figs 15a)** and **b)** compare the baseline geometry using the TT and TRS boundary conditions. The plots are at slightly different relative circumferential positions between the rotor and diffuser, but the results are in very good qualitative agreement. Comparing the results from the two radius ratios with the TT calculation (**figs 15a** and **c)**) the peak Mach number experienced by the diffuser vanes is actually similar, locally just above 1.2 at the diffuser inlet, and this decreases with radius to the diffuser leading edge.

The unsteady interactions lead to a slightly higher Mach number in the semi-vaneless space of every third or fourth diffuser vane, with an unsteady expelled shock standing clear of the diffuser leading edge on the adjacent suction surface. The area of highest absolute Mach number represents the wakes leaving the impeller. The vector addition of this low relative velocity and the blade speed results in high Mach number in the absolute frame.

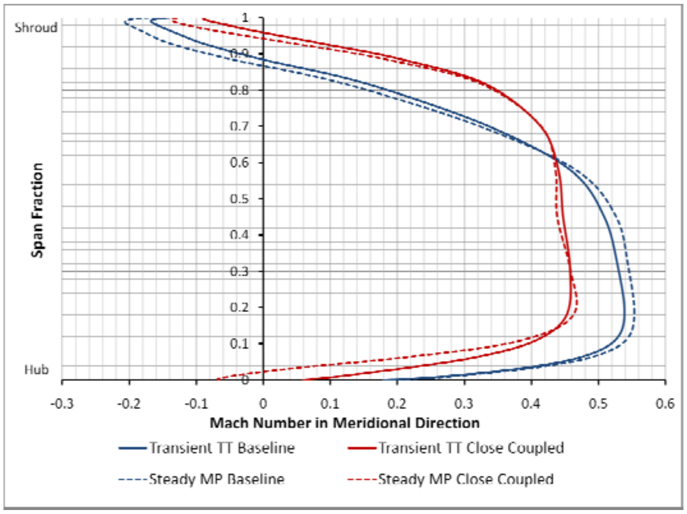

Figure 16 Average Meridional Mach Number at the impeller-diffuser interface

Fig 16 compares profiles of meridional Mach number at the impeller-diffuser interface of the baseline and close coupled cases for both the TT and steady calculations. In this impeller there is clearly an area of reversed flow close to the casing, representing a high blockage in this narrow flow channel. In order to design the stage with the correct matching between the two rows, it is probably more important to capture this blockage accurately than it is to predict the unsteady effects. The boundary of the flow reversal in the steady calculation is circumferentially constant due to the stage interface, but this occurs at a similar spanwise location to that of the unsteady TT simulation, even though this is not circumferentially averaged. The good agreement between these results in terms of blockage prediction illustrates why the steady stage calculation is so useful in giving accurate predictions of the main interaction between the components as designs are developed. A simulation without this reverse flow feature at the interface would not be useful to compute the matching of the components: it would lead to incorrect performance curves and matching as the diffuser would not have the correct blockage at inlet and would pass more flow.

A further impression of the time evolution of the flow in the TT calculation can be seen in **fig 17** for the 15% gap simulation. The impeller exit relative Mach number is shown and the difference between the Mach number distribution and wakes at the impeller outlet vary little as the impeller rotates past the diffuser leading edges.

Similar results were found for the closely spaced diffuser vanes, and are not shown here. In this impeller the wake clearly appears to be stronger on the splitter blades than on the main blades, suggesting room for further optimization potential if the splitter were to have a different shape than the main blade, see Came and Robinson **[18]** and Lohmberg et al. **[19]** for example.

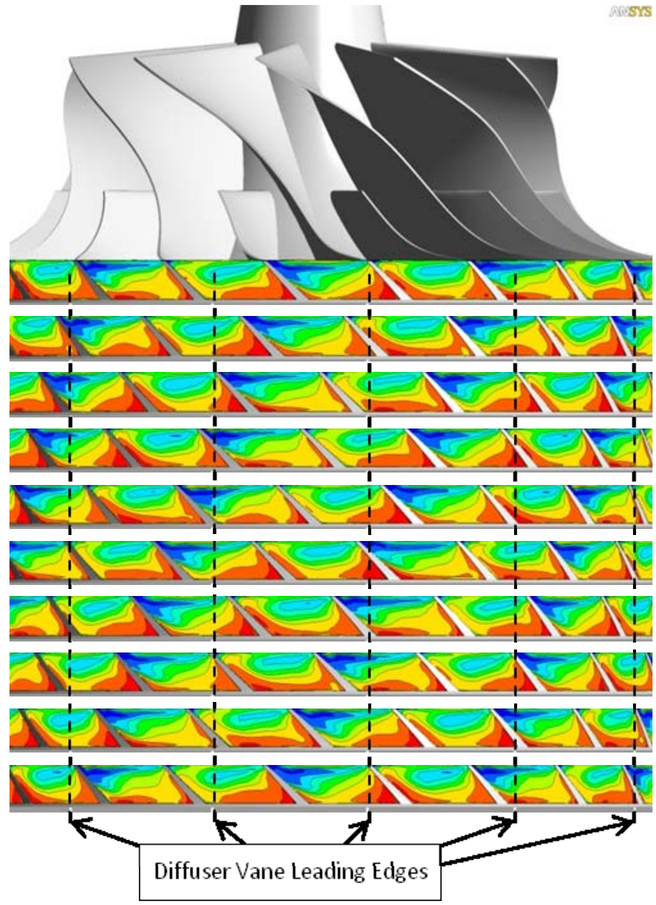

Figure 17 Time evolution of the relative Mach number at impeller outlet in the TT calculation with a diffuser radius ratio of 115%

DISCUSSION

The work reported here was mainly to investigate the practicality of TT calculations to supplement, or perhaps to replace, the stage interface in the design process of compressor stages. The stage interface has been a very effective and pragmatic approach to design over many years and the authors have confidence in its validity at the typical levels of impeller-diffuser spacing used in most applications.

It does not provide the unsteady pressure information useful for forced response analysis but, at the larger spacing, experience has shown that so long as reasonable care is taken to avoid obvious excitation of natural frequencies, the design should not be susceptible to high cycle fatigue failure from diffuser interaction.

That the stage interface appeared also to work well with the reduced gap was a useful finding of this work. The implementation of a stage interface which includes the possibility of reverse flow across this plane is clearly a crucially important aspect of impeller-diffuser interaction calculations. The authors have little previous experience in designing at small gaps, but clearly this can be successfully computed using the stage interface. At lower levels of tip-speed where the stress levels are less important, this may be a useful benefit if efficiency can be accrued with no significant increased risk of fatigue failure.

The diffuser designed for the reduced gap was not particularly optimized in the design procedure used, as the main effort was to examine the use of the stage interface at reduced gaps that had previously not seriously been studied by the authors.

However, an efficiency increment was predicted, which is in line with the literature already discussed. Whether this came specifically from the interaction process is difficult to isolate. Even with the best of intentions it is difficult to arrange a 'back-to-back' test when so many factors are involved: throat area, vane incidence, camber distribution, meridional channel shape are all involved. A useful follow-on project would be to redesign both diffusers within the same overall diameter constraint, but otherwise freely optimized.

It is difficult to be precise about the computing requirements of the various runs since they were carried out over a range of different machines. However, a rough idea can be obtained simply based on the total number of iterations/coefficient loops multiplied by the grid size, assuming 300 iterations for the stage calculation and 3 coefficient loops per timestep over 20 rotor periods with 34 timesteps per rotor passage for the transient. The relative efforts are approximated as follows:

- Steady (Stage Interface): 0.10
- Time Transformation (TT): 1.00
- Full Transient (TRS): 5.56

Bearing in mind these data and the results reported above, the steady approach still has its place in developing optimal aerodynamic designs even at relatively close spacing. TT comes to the fore when unsteady mechanical effects are important and the significant time-saving over TRS seems attractive at today's levels of computing capacity.

CONCLUSIONS

An excellent validation of overall performance has been obtained on a high Mach number compressor stage using the steady Stage Interface model with the SST turbulence model and a moderate grid density for a case with 'standard' impeller diffuser spacing of 115%. This demonstrates the suitability of this approach for design iterations. A key aspect of this is shown to be the ability of the current implementation of the stage interface to accept flow in both directions across the interface.

The stage interface has also been found to work stably down to an impeller diffuser spacing of 107%.

The reduced gap design yielded an efficiency improvement when analysed using the TT approach, but steady analysis found no increment.

The TT transient analysis has given comparable results to the full 360° TRS approach at standard levels of spacing with much reduced computational effort. This yields the time-dependent pressure data that are needed for forced response structural analysis and identifies an increase in the impeller outlet pressure fluctuation at a suitable location of 116% for the closely spaced diffuser.

ACKNOWLEDGMENTS

The authors wish to acknowledge the kind support of ABB Turbo Systems AG who provided the test data and gave permission to use the geometry of the compressor stage for this computational study.

The assistance of Dr. Rubens Campregher of ANSYS with some of the unsteady calculations is also gratefully acknowledged.

REFERENCES

[1] Dean, R., and Senoo, Y., 1960, ''Rotating Wakes in Vaneless Diffusers'', ASME J. Basic Eng., 82, pp. 563–574.
[2] Zangeneh, M., Amarel, N. Daneshkhah, K. and Krain, H., (2011). "Optimization of 6.2:1 Pressure Ratio Centrifugal Compressor Impeller by 3D Inverse Design", Proceedings of the ASME Turbo Expo 2011, GT2011-46505.
[3] Benetschik, H. and Eisenbach, S. "Potential of 3D diffuser vanes inside compressors of exhaust gas turbochargers for two-stage turbocharging applied to large Diesel engines", 16th Supercharging Conference, Dresden 29th-30th September 2011.
[4] Cumpsty, N., 1989, *Compressor Aerodynamics*, Longman Scientific and Technical, Essex, England.
[5] Rodgers, C., (1982). "The Performance of Centrifugal Compressor Channel Diffusers", ASME Paper No. 82-GT-10.
[6] Shum, Y. K. P., Tan, C. S., and Cumpsty, N.A., (2000) "Impeller-diffuser interaction in a centrifugal compressor, Trans ASME Jnl. of Turbomachinery, Vol: 122, Pages: 777 – 786.
[7] Ziegler, K. U., Gallus, H. E. and Niehuis, R., (2003) "A study on Impeller-Diffuser Interaction – Part I: Influence on the Performance", Trans ASME Jnl. of Turbomachinery, Vol: 125, Pages: 173 – 182.
[8] Ziegler, K. U., Gallus, H. E. and Niehuis, R., (2003) "A study on Impeller-Diffuser Interaction – Part II: Detailed Flow Analysis", Trans ASME Jnl. of Turbomachinery, Vol: 125, Pages: 183 – 192.
[9] ANSYS CFX Version 14.0, ANSYS Inc., 2011.
[10] Denton, J.D. "The calculation of three-dimensional viscous flow through multistage turbomachines" Trans. ASME Journal of Turbomachinery, Vol 114, pages 18-26.
[11] Biesinger, T., Cornelius, C., Rube, C., Schmid, G, Braune, A., Campregher, R., Godin, P., and Zori, L, (2010), "Unsteady CFD Methods in a Commercial Solver For Turbomachinery Applications", Proceedings of the ASME Turbo Expo 2010, GT2010-22762

[12] Galpin, P.F., Broberg, R.B. and Hutchinson, B.R., "Three-Dimensional Navier Stokes Predictions of Steady State Rotor/Stator Interaction with Pitch Change", Third Annual Conference of the CFD Society of Canada, June 27-27, 1995, Banff, Alberta, Canada
[13] Sick, M., Drtina, P. and Casey, M.V., (1998), "The use of stage capability in CFD for turbomachinery, with application in a Francis turbine", International Journal of Computer Applications, Vol. 11 Nos 3/4/5, pp 219-220, 1998
[14] Giles, M., 1988, "Calculation of Unsteady Wake/Rotor Interaction", Journal of Propulsion and Power, 4(4), pp. 356–362
[15] Menter, F.R., 1994, "Two-equation eddy-viscosity turbulence models for engineering applications", AIAA-Journal, 32, (8), pp. 1598 – 1605
[16] Cukurel, B., Lawless, P.B. and Fleeter, S., (2008), "PIV investigations of a high speed centrifugal compressor diffuser: spanwise loading variations", ASME Turbo Expo 2008, Berlin, ASME paper GT2008-51321
[17] Connell, S., Braaten, M., Zori, L., Steed, R., Hutchinson, B. and Cox, G. "A Comparison of Advanced Numerical Techniques To Model Transient Flow in Turbo-machinery Blade Rows" Proceedings of ASME Turbo Expo 2011, GT2011-45820.
[18] Came, P. M. and Robinson, C. J. (1999), "Centrifugal compressor design", IMechE Journal of Mechanical Engineering Science, Vol. 213, No C2, pp 139-156.
[19] Lohmberg, A., Casey, M., Ammann S., (2003), "Transonic Radial Compressor Inlet Design", Proc. Instn. Mech. Engrs., Vol. 217, J. Power and Energy, 2003.